International Journal of Neural Systems, Vol. 0, No. 0 (2005) 1–??

EVALUATION OF BRAIN FUNCTIONAL CONNECTIVITY FROM ELECTROENCEPHALOGRAPHIC SIGNALS UNDER DIFFERENT EMOTIONAL STATES

BEATRIZ GARCÍA-MARTÍNEZ
Departamento de Sistemas Informáticos, Escuela Técnica Superior de Ingenieros Industriales, Universidad de Castilla-La Mancha, 02071-Albacete, Spain
Instituto de Investigación en Informática de Albacete, Universidad de Castilla-La Mancha, 02071-Albacete, Spain
E-mail: Beatriz.GMartinez@uclm.es

ANTONIO FERNÁNDEZ-CABALLERO
Departamento de Sistemas Informáticos, Escuela Técnica Superior de Ingenieros Industriales, Universidad de Castilla-La Mancha, 02071-Albacete, Spain
Instituto de Investigación en Informática de Albacete, Universidad de Castilla-La Mancha, 02071-Albacete, Spain
CIBERSAM (Biomedical Research Networking Centre in Mental Health), Madrid, Spain

ARTURO MARTÍNEZ-RODRIGO
Research Group in Electronic, Biomedical and Telecommunication Engineering, Facultad de Comunicación, Universidad de Castilla-La Mancha, 16071-Cuenca, Spain
Instituto de Tecnologías Audiovisuales de Castilla-La Mancha, Universidad de Castilla-La Mancha, 16071-Cuenca, Spain

RAÚL ALCARAZ
Research Group in Electronic, Biomedical and Telecommunication Engineering, Escuela Politécnica de Cuenca, Universidad de Castilla-La Mancha, 16071-Cuenca, Spain

PAULO NOVAIS
Algoritmi Center, Department of Informatics, Universidade do Minho, 4800-058 Guimarães, Portugal

The identification of the emotional states corresponding to the four quadrants of the valence/arousal space has been widely analyzed in the scientific literature by means of multiple techniques. Nevertheless, most of these methods were based on the assessment of each brain region separately, without considering the possible interactions among different areas. In order to study these interconnections, the present study computes for the first time the functional connectivity metric called cross-sample entropy for the analysis of the brain synchronization in four groups of emotions from electroencephalographic signals. Outcomes reported a strong synchronization in the interconnections among central, parietal and occipital areas, while the interactions between left frontal and temporal structures with the rest of brain regions presented the lowest coordination. These differences were statistically significant for the four groups of emotions. All emotions were simultaneously classified with a 95.43% of accuracy, overcoming the results reported in previous studies. Moreover, the differences between high and low levels of valence and arousal, taking into account the state of the counterpart dimension, also provided notable findings about the degree of synchronization in the brain within different emotional conditions and the possible

implications of these outcomes from a psychophysiological point of view.

Keywords: Electroencephalography; Functional connectivity; Cross-sample entropy; Emotions recognition.

1. Introduction

The interest in the study of the brain has considerably increased in the last decades with the purpose of completely evaluating its functioning under a wide variety of health and environmental circumstances.[1] Traditional methods have been focused on the association of a particular mental process or function with a determined anatomical region, thus considering brain structures as independent and unconnected systems.[2] However, the existence of interconnections between different structures has been demonstrated, hence suggesting that the brain works as a network in which the information is shared among separate areas for the development of cognitive tasks.[3]

The connectivity in the brain can be anatomical (given by the physical and structural links between distinct areas) and functional (referring to the statistical dependencies among non-physically linked regions).[4] In the second case, the existence of functional networks entails a synchronized behavior between separate brain structures for the development of mental tasks.[3] Therefore, it is crucial to evaluate the regional interactions for a proper and complete description of the information processing dynamics of the brain.[3]

The assessment of brain functional connectivity has been addressed in the scientific literature through different mathematical methodologies.[5,6] Nonetheless, the interactions between neurons and brain structures present a nonlinear and nonstationary nature, thus the application of nonlinear metrics, like cross-mutual information, transfer entropy, or permutation dissalignment index, among others, could complement the information reported by linear techniques and thus allow to completely characterize connectivity and functional interactions among separate brain areas. Indeed, these nonlinear functional connectivity techniques have provided relevant information for the diagnosis of mental disorders such as Alzheimer,[7,8] depression,[9] Parkinson,[10] mild cognitive impairment[11] or autism,[12,13] among others. In the same manner, some studies have also evaluated the performance of these connectivity metrics for emotions recognition.[14,15]

Another interesting functional connectivity index is the well-known cross-sample entropy (CSE). This metric evaluates the coordination between different brain regions by means of the estimation of the repetitiveness of patterns within two brain signals recorded at different brain areas, thus revealing the degree of similarity of the dynamics and the synchronized performance of separate brain structures.[16] The CSE index has already been computed by our research group for the recognition of two emotions, concretely calm and distress.[17] Nevertheless, to the best of our knowledge, this metric has never been used for the evaluation of more than two emotional states. In the scientific literature, the four groups of emotional states corresponding to the four quadrants of the circumplex model of emotions proposed by Russell have been typically analyzed with various methodologies. According to this scheme, all emotions can be distributed in a bi-dimensional space in terms of their associated level of valence (pleasantness or unpleasantness) and arousal (activation or relaxation).[18] Then, the four quadrants of this emotional space are HAHV (high arousal/high valence), HALV (high arousal/low valence), LAHV (low arousal/high valence) and LALV (low arousal/low valence), as can be observed in Figure 1.

Figure 1. Representation of the circumplex model of emotions proposed by Russell, including the four groups of emotions studied in this work.

The present study computes CSE for the first

time to discern between the four groups of emotions corresponding with the four quadrants of the valence/arousal space and reveal the degree of coordination between brain areas under these emotional conditions. The assessment will be firstly done by means of a multiclass approach in which the four groups of study are considered simultaneously. In addition, the differences between the four groups of emotions will also be studied by means of comparing them two by two in four binary-class schemes for the analysis of different levels of valence and arousal separately. In fact, both emotional dimensions are strongly interrelated, thus influencing one on the other and being necessary to jointly consider valence and arousal levels.[19] For this reason, the evaluation of high and low levels of one emotional dimension will be carried out taking into account a fixed level of the counterpart dimension, with the purpose of evaluating the synergy between valence and arousal. The results could report new insights about the relationships between brain regions and the degree of synchronized activity produced in the brain under the different emotional conditions under study.

This manuscript is structured as follows. Section 2 describes the database and the preprocessing process, together with the mathematical definition of CSE, the experimental procedure and the statistical analyses and classification processes conducted. Later, results are presented in Section 3 and subsequently discussed in Section 4. Finally, the main conclusions of this study are included in Section 5.

2. Materials and Methods

2.1. *Database*

The EEG signals assessed in this study were contained in the Database for Emotion Analysis using Physiological Signals (DEAP).[20] This publicly available dataset contains a total of 1,280 samples of different emotional states from 32 healthy participants with ages ranging between 19 and 37 years old (mean age 26.9, 50% male). More precisely, these subjects visualized 40 videoclips with emotional content of 1-minute of duration, while EEG from 32 channels and other physiological signals were acquired. After each videoclip, participants rated their emotional state indicating the level of valence (pleasantness-unpleasantness) and arousal (activation-relaxation) produced by the stimulus in a scale from 1 to 9.

The samples in the DEAP database included all emotions contained in the valence/arousal space. Nevertheless, only a subset of those samples was chosen in this work and distributed in four groups: HAHV (arousal and valence ≥ 6), HALV (arousal ≥ 6 and valence ≤ 4), LAHV (arousal ≤ 4 and valence ≥ 6) and LALV (arousal and valence ≤ 4). The samples in the borderline among two groups were not considered, thus only the samples corresponding with a strongly elicited emotion were finally analyzed in this study. Hence, the number of samples included in each group was HAHV = 267, HALV = 101, LAHV = 154 and LALV = 124. The range of values and mean level of valence and arousal for each group of emotions is shown in Table 1.

Table 1. Range, mean and standard deviation of valence and arousal levels for each group of emotions.

	Arousal		**Valence**	
	Range	**Mean±Std**	**Range**	**Mean±Std**
HAHV	[6-9]	7.08±0.80	[6-9]	7.51±0.87
HALV	[6-9]	7.08±0.90	[1-4]	2.37±0.97
LAHV	[1-4]	2.92±0.81	[6-9]	7.08±0.74
LALV	[1-4]	2.49±0.95	[1-4]	2.71±0.93

2.2. *Preprocessing of EEG recordings*

The EEG recordings included in DEAP database were acquired with 32 channels located over the scalp according to the international standard 10-20 scheme for electrodes distribution.[21] Prior to the application of any kind of analysis, EEG signals were preprocessed and filtered by means of EEGLAB, a toolbox for Matlab specifically created for the assessment of EEG recordings.[22] Signals were firstly downsampled from 512 Hz to 128 Hz and re-referenced to the average potential of all channels by removing this mean potential from each single EEG electrode.[23] This re-referencing technique is one of the most used methods for EEG preprocessing because of its computational simplicity and its ability to reduce noise through the average process.[23] Later, two forward/backward high-pass and low-pass filters with cutoff frequencies of 3 and 45 Hz, respectively, were applied to eliminate the frequencies out of the bands in the EEG spectrum containing emotional information.[24] These filtering approaches also removed baseline and power line interferences. In addition, noise

and other interferences that remained after the previous preprocessing steps were eliminated by means of an independent component analysis (ICA). Concretely, it was used for the rejection of artifacts derived from both physical (such as eye blinks, facial movements or heart bumps) and technical sources (like bad contacts of the electrodes with the scalp, or electrode-pops). The application of ICA consisted of the computation of the independent components and the posterior removal of those containing artifactual information, thus only remaining the data related to the brain activity. Finally, electrodes contaminated with high-amplitude noise were removed and reconstructed through the interpolation of adjacent channels.[25]

The videoclips used in the DEAP experiment had a duration of 60 seconds.[20] Nevertheless, only the last 30 seconds of each trial were finally analyzed in this study with the purpose of ensuring that the target emotion had been strongly elicited.[20] The original time series x were normalized and named as y, such that the effect of amplitude in the comparison between EEG electrodes was eliminated:

$$y = \frac{x - \bar{x}}{\sigma}, \tag{1}$$

being $\bar{x}$ and σ the mean and standard deviation of each signal x, respectively. Normalized signals y were then divided into six equally-sized non-overlapped segments of 5 seconds ($N = 3840$ samples per segment). Then, CSE was computed for each segment, evaluating the similarity of patterns between each channel and the rest of EEG electrodes. Finally, the value of CSE for each pair of channels was computed as the average of the outcomes obtained for the six segments.

2.3. *Cross-Sample Entropy (CSE)*

CSE represents an improvement of cross-approximate entropy in terms of its relative consistency for different conditions.[26] Precisely, CSE is based on the comparison of signals from two different yet intertwined variables for the assessment of their level of asynchrony or dissimilarity.[26,27] Hence, it is possible to evaluate the evolution of feedback, control, and other characteristics of a system, without the necessity of modeling the underlying system.[27] In addition, as CSE analyzes both dominant and secondary patterns in the time series, it allows to quantify changes in the underlying dynamics that cannot be reported by peak occurrences or amplitudes.[28] More concretely, having two signals $x_1(n)$ and $x_2(n)$ of N samples of length, CSE evaluates the conditional regularity or frequency of patterns from $x_1(n)$ that are similar to patterns from $x_2(n)$ of windows length m within a tolerance r. This can be better observed in Figure 2, which shows the search of patterns of length $m = 3$ along the time series $x_2(n)$ that match with a reference pattern of the same length from the signal $x_1(n)$ within a tolerance r. Therefore, considering two brain signals $x_1(n)$ and $x_2(n)$ from separate brain regions provides the degree of synchronization among both areas. Larger CSE values represent a greater level of asynchrony between both time series, thus indicating less pattern matches.[26]

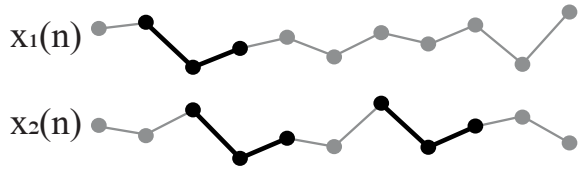

Figure 2. Representation of the performance of CSE index for evaluating the degree of coordination among two brain signals $x_1(n)$ and $x_2(n)$ from separate brain regions.

For the computation of CSE, $N - m$ vectors of length m samples are firstly formed from $x_1(n)$ and $x_2(n)$,[26] thus

$$\mathbf{X}^m_{1,i} = \{x_1(i), x_1(i+1), \ldots, x_1(i+m-1)\}, \tag{2}$$

$$\mathbf{X}^m_{2,j} = \{x_2(j), x_2(j+1), \ldots, x_2(j+m-1)\}, \tag{3}$$

where i and j are both in the range $[1, N-m]$. These vectors are the representation of m consecutive x_1 and x_2 samples starting at i-th and j-th points, respectively. Then, the maximum absolute difference in the scalar components of $\mathbf{X}^m_{1,i}$ and $\mathbf{X}^m_{2,j}$ represents the distance d^m_{ij} between both vectors:

$$\begin{aligned} d^m_{ij} &= d[\mathbf{X}^m_{1,i}, \mathbf{X}^m_{2,j}] = \\ &= \max_{k \in (0, m-1)} |x_1(i+k) - x_2(j+k)|. \end{aligned} \tag{4}$$

Hence, the probability of having patterns in x_2 that are similar to a pattern in x_1 of window length m within a tolerance r is represented as

$$\phi^m(r)(x_1||x_2) = \\ = \frac{1}{N-m}\sum_{i=1}^{N-m}\Big(\frac{1}{N-m}\sum_{j=1}^{N-m}\Theta\big(r-d_{ij}^m\big)\Big), \quad (5)$$

being $\Theta(x)$ the Heaviside function, with the following mathematical definition:[26]

$$\Theta(x) = \begin{cases} 1, \text{ if } x \geq 0, \\ 0, \text{ if } x < 0. \end{cases} \quad (6)$$

In the same manner, the probability is also estimated for patterns of length $m+1$:

$$\phi^{m+1}(r)(x_1||x_2) = \\ \frac{1}{N-m}\sum_{i=1}^{N-m}\Big(\frac{1}{N-m}\sum_{j=1}^{N-m}\Theta\big(r-d_{ij}^{m+1}\big)\Big). \quad (7)$$

CSE is then calculated as the negative natural logarithm of the conditional probability ϕ^{m+1}/ϕ^m:[26]

$$\mathrm{CSE}(m,r,N)(x_1||x_2) = \\ -\lim_{N\to\infty}\Big(\ln\frac{\phi^{m+1}(r)(x_1||x_2)}{\phi^m(r)(x_1||x_2)}\Big), \quad (8)$$

As the length of the time series N is finite, CSE is finally computed as[26]

$$\mathrm{CSE}(m,r,N)(x_1||x_2) = -\ln\frac{\phi^{m+1}(r)(x_1||x_2)}{\phi^m(r)(x_1||x_2)}. \quad (9)$$

It is important to remark that this metric is direction independent, which means that $\mathrm{CSE}(m,r,N)(x_1||x_2)$ is equal to $\mathrm{CSE}(m,r,N)(x_2||x_1)$. It is because ϕ^m simply considers the number of pairs of vectors from the two signals matching within r, independently of which signal is the template and which is the target.[26] As it occurs in the case of sample entropy, the proper selection of parameters m and r is essential for correctly determining the CSE value. Therefore, as there are no guidelines for an optimization of those values, the widely recommended parameters $m = 2$ and $r = 0.2$ were finally chosen in the present work.[16]

2.4. *Experimental approaches and statistical analysis*

The normality and homoscedasticity of the distribution of samples was corroborated by Shapiro-Wilks and Levene tests, respectively, thus it is possible to represent the final results as mean±standard deviation for every pair of EEG channels. Precisely, the mean and standard deviation of CSE was computed for each pair of channels in each of the four groups of emotions. In addition, an analysis of variance (ANOVA) was used to check the possible statistical differences among the interactions between channels with the strongest and the weakest level of coordination within each group of study separately. It should be remarked that only statistical significance results of $\rho < 0.05$ were considered as significant.

The four quadrants of the emotional model were also assessed together by means of two different analyses. The first case consisted of a multiclass scheme for the simultaneous assessment of the four groups of emotions under study. For that purpose, an ANOVA test was conducted for the quantification of the capability of CSE to statistically discern between the four emotional classes corresponding to the four quadrants of the valence/arousal model. On the other hand, a binary-class approach was developed for the identification of the different groups of emotions two by two, according to their values of valence and arousal separately. However, the differences between high and low levels of one emotional dimension were evaluated also taking into account a fixed value of the other dimension. As a result, the detection of high and low levels of valence was conducted for a fixed high arousal (HAXV; HAHV vs. HALV) and for a fixed low arousal (LAXV; LAHV vs. LALV). In the same manner, high and low levels of arousal were discerned for a fixed high valence (XAHV; HAHV vs. LAHV) and for a fixed low valence (XALV; HALV vs. LALV). Therefore, the four quadrants were evaluated two by two in a total of four binary schemes, according to their levels of both emotional dimensions. For the four cases, a one-way ANOVA test was also applied for the assessment of the statistical differences between the CSE values of the groups of study in each binary approach.

2.5. *Classification procedure*

With the aim of discerning among the four groups of emotions, a support vector machine (SVM) classification scheme was developed. Firstly, all samples in the dataset of study were firstly rearranged using a 10-fold cross-validation approach to avoid the overfitting of the classifiers. Hence, samples were ran-

domly redistributed in 10 equally-sized folds ensuring the representativity of each group of emotions with respect to the whole dataset. For each iteration of the cross-validation process, nine folds were used to train the classifier and the remaining one for testing it, such that after the ten rounds all folds were used for both training and testing. In each step, a sequential forward selection (SFS) was used. This features reduction strategy sequentially selects the most relevant observations for the prediction of data, including one feature at each step of the algorithm until there is no improvement in prediction, thus obtaining the subset of features that provide the best information.[29] In this case, SFS was applied for the selection of the subset of pairs of EEG channels minimizing the misclassification rate of the SVM classifier. The SVM model implemented in this study presented a Gaussian kernel with a scale factor of 0.35 and a box constraint of 1. Then, the pairs of channels selected by the SFS approach were used as input features to train the SVM classifier with the nine folds reserved for training, and the resulting model was finally tested with the remaining fold.

The assessment of the efficiency of the SVM model obtained in each iteration of the cross-validation approach was made with respect to the true positive (TP, positive samples correctly labeled as positive), true negative (TN, negative samples properly identified as negative), false positive (FP, negative samples incorrectly labeled as positive) and false negative (FN, positive samples incorrectly detected as negative) cases. In the multiclass approach, different performance indices were applied considering these parameters. The first one was the precision (P), or positive predictive value, representing the probability of properly making a correct positive classification:

$$P = \frac{TP}{TP + FP} \tag{10}$$

In addition, recall (R) represents the sensitiveness of the model to detect the class considered as positive:

$$R = \frac{TP}{TP + FN} \tag{11}$$

On the other hand, accuracy (Acc) considers all the correctly detected cases assigning the same importance to all of them:

$$Acc = \frac{TP + TN}{TP + TN + FP + FN} \tag{12}$$

Nevertheless, in the case of an imbalanced number of samples among different groups, the F_1-score parameter gives a global measurement of accuracy more precise than Acc for the evaluation of the models, using P and R values for its computation.

$$F_1 = 2 * \frac{P * R}{P + R} = \frac{2 * TP}{2 * TP + FP + FN} \tag{13}$$

On the other hand, the binary-class schemes evaluated the performance of the classification model according to its sensitivity (Se), specificity (Sp) and Acc. Concretely, Se is the proportion of TP out of all positives, and its mathematical expression is the same as for R (eq. 11). On the other hand, Sp is the percentage of TN out of all negatives:

$$Sp = \frac{TN}{TN + FP} \tag{14}$$

3. Results

3.1. *Average levels of CSE*

As CSE is computed for each pair of EEG channels, results obtained for each trial can be represented by a 32 × 32 symmetric matrix that shows the relationship of each channel with the rest of electrodes. According to the color scale used for the representation of CSE outcomes, blue-colored squares are those with the lowest values, indicating a strongly coordinated activity and highly similar dynamics between the two corresponding brain areas. On the contrary, red colors are used for the representation of the highest CSE results, thus depicting the most dissimilar and asynchronized dynamics between brain regions. In addition, the main diagonal represents the interaction of one channel with itself, which is not applicable with CSE and, therefore, is represented with white squares.

For each of the four groups of emotions, the average of CSE from all samples was computed and represented in Figure 3. As can be seen, the strongest synchronization (given by the lowest CSE values) appeared in central, parietal and occipital regions in all the cases. More precisely, this highly coordinated activity was present in the interactions between those regions within the same hemisphere (intra-hemispheric connections) and among the same

areas from both hemispheres (inter-hemispheric connections). On the contrary, the most asynchronized behavior (represented by the highest CSE levels) appeared in the connections between frontal and temporal channels from left hemisphere with the rest of brain regions. With respect to the standard deviation of CSE values obtained for each group, results ranged between 0.04 and 0.16, compared with mean values, which ranged between 0.55 and 0.85, such as Figure 3 shows. These results represent a reduced dispersion of the samples within each group.

For a better understanding of the anatomical implications of these coordination results, Figure 4 shows the interactions with (a) the strongest coordination (lowest CSE values) and (b) the weakest synchronization (highest CSE results) in a brain model. In general terms, the four groups of emotions presented similar synchronization tendencies aforementioned, therefore these two models are representative of all the emotional conditions studied in this work. In addition, an ANOVA analysis was applied for the evaluation of the statistical differences among the interactions with the strongest and the weakest level of coordination in each group separately. This analysis corroborated the similarities among the four groups, reporting statistically significant outcomes for the comparison among interactions including left frontal and temporal regions (weakest coordination levels) with interconnections between other brain areas, especially those involving regions from the posterior half of the brain from both hemispheres (strongest coordination levels). This reinforces the existence of notable differences in the coordination level among the pairs of brain regions with the weakest and the strongest synchronization.

Although in general terms the four groups of emotions presented similar synchronization tendencies aforementioned, the level of synchronization slightly varied for each group. More concretely, the groups of HALV (Figure 3(a)) and LAHV (Figure 3(d)) presented a generalized decrease of CSE levels, especially in the intra- and inter-hemispheric interactions between posterior areas of the brain, represented by a higher presence of blue colors in these regions. Therefore, the brain showed a more self-coordinated functioning and more similar dynamics among all areas under the corresponding emotional states, which are fear, distress or anger in the group of HALV, and calmness or relaxation in the group of LAHV.

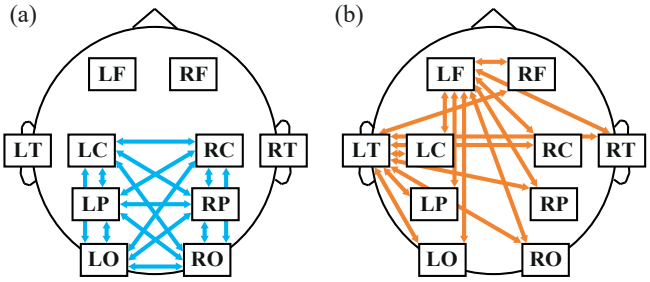

Figure 4. Representation of interactions with (a) the strongest synchronization (lowest CSE values) and (b) the weakest synchronization (highest CSE results) for the general tendency of the four groups of emotions.

3.2. *Multiclass analysis*

The statistical analysis for the simultaneous assessment of the four groups of emotions revealed statistically significant results for 14 out of 496 possible pairs of channels, including the intra-hemispheric interactions between left frontal region with itself and with parieto-occipital channels, and the interactions among fronto-central and centro-parietal regions in right hemisphere. The inter-hemispheric interactions among left and right frontal areas also reported statistically significant outcomes. On the other hand, the SFS approach selected a total of 42 interactions in the 10 iterations of the cross-validation process. The brain regions involved in these interactions chosen were also those with statistically significant results in ANOVA analysis, i.e., left frontal with left frontal and parieto-occipital, left frontal with right frontal, and right fronto-central and centro-parietal regions.

The 42 pairs of channels selected by the SFS were used as input features in the SVM classification model in each iteration of the cross-validation scheme. Final performance results were obtained as the average of the ten iterations and are shown in Table 2. As can be observed, the global accuracy for the simultaneous classification of the four groups of emotions is 95.43%. The two groups with low valence (i.e., HALV and LALV) present the highest precision (97.89 and 98.32%, respectively), whereas the groups with high valence (HAHV and LAHV) provide the highest recall values (98.95 and 93.51%, respectively). Finally, the average F_1 was 94.43%,

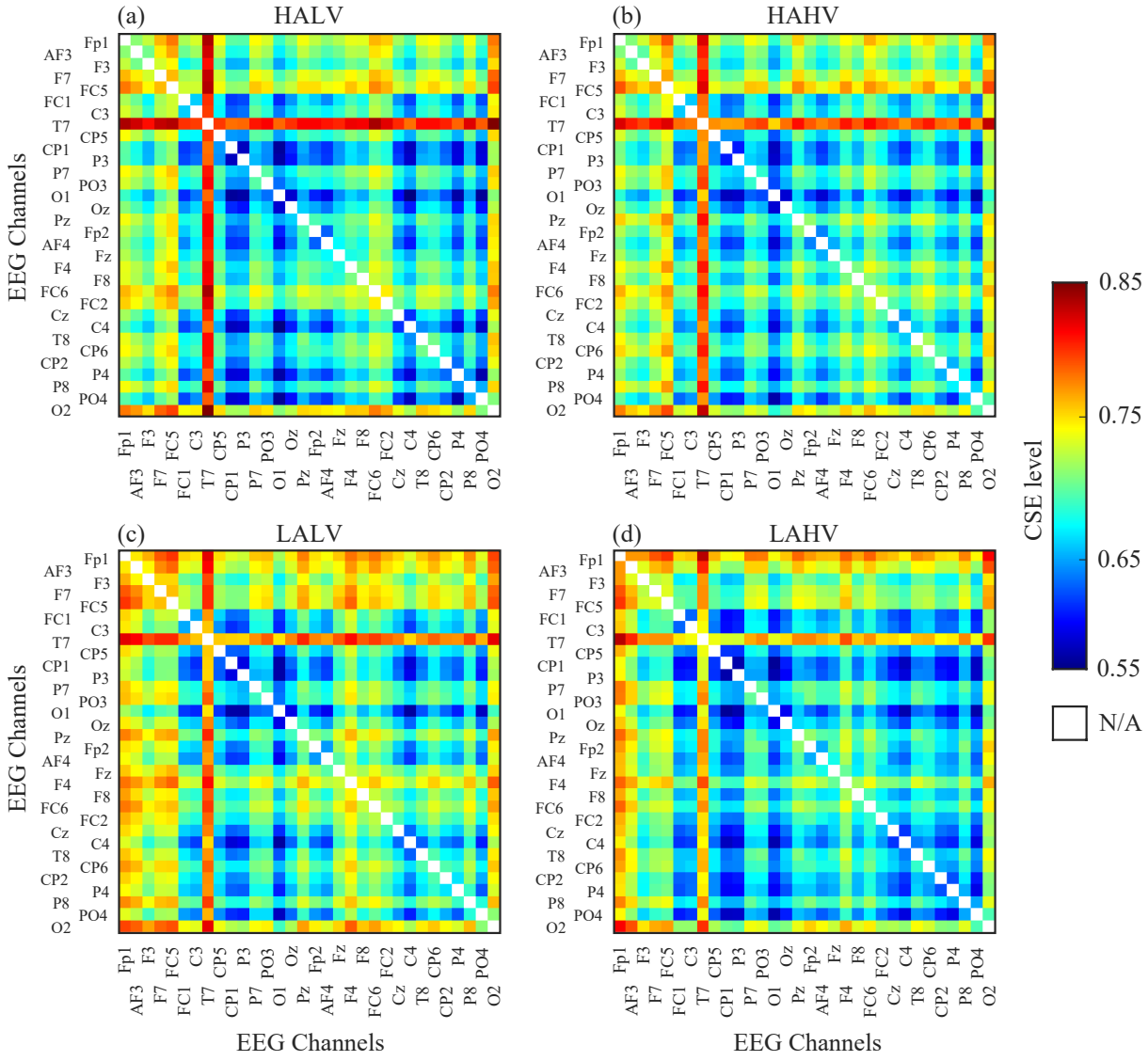

Figure 3. Average CSE levels from all pairs of EEG channels in the four groups of emotions under study.

being HAHV and LALV the groups with the best results, over 95% in both cases.

Table 2. Performance of CSE in multiclass analysis.

Group	Acc	P	R	F_1
HAHV	95.60%	92.15%	98.95%	95.33%
HALV	95.40%	97.89%	88.12%	92.59%
LAHV	95.14%	95.70%	93.51%	94.56%
LALV	95.60%	98.32%	92.66%	95.26%
Average	95.43%	96.01%	93.31%	94.43%

3.3. *Binary-class analysis*

The differences of CSE values between two groups of emotions can be depicted using a similar representation as in the case of mean CSE levels. In this case, each element of the 32 × matrix is the representation of the difference of CSE among the two emotions under study for the corresponding pair of channels. With this respect, the interpretation of the color scale is different. In this case, if the difference of CSE between two emotions A and B is obtained as CSE(A)-CSE(B), then the map of differences indicates with red colors those pairs of channels with greater CSE in emotion A than in emotion B (i.e.,

positive difference), whereas blue colors are used for marking the pairs of electrodes with a higher value of CSE in emotion B than in emotion A (i.e., negative difference). Finally, green squares represent the pairs of EEG channels with negligible differences between both emotional states.

The differences of average levels of CSE between pairs of emotional groups are represented in Figure 5. Precisely, Figures 5(a) and (b) are the CSE level of high valence minus low valence when having a fixed high and low arousal, namely HAXV and LAXV, respectively. In the same manner, Figures 5(c) and (d) represent XAHV and XALV schemes, which correspond with the result of CSE in high arousal minus CSE in low arousal when the valence is fixed to low and high level, respectively. Therefore, each difference map has been obtained as the high minus the low level of the variable emotional dimension (either valence or arousal) when the other dimension has a fixed level.

In the cases of HAXV and LAXV schemes, represented in Figures 5(a) HAHV-HALV and (b) LAHV-LALV, it can be observed that the highest differences appear in the interactions between the right hemisphere with all the brain regions within the same hemisphere and also with the counterpart. However, the CSE value is higher (more dissimilarity) in those interactions for high valence than for low valence when having a fixed high arousal, which is represented by red colors in Figure 5(a). On the contrary, the same interactions are represented in color blue when the arousal is fixed to a low level (Figure 5(b)), thus being CSE higher (and the coordination lower) for low valence than for high valence in these interconnections. In the latter case, the differences in the interactions between left and right prefrontal channels with left parieto-occipital areas are also relevant, but colored with red and orange, thus depicting a higher level of CSE (lower coordination) for high valence than for low valence.

With respect to the statistical analyses, in HAXV scheme only the interaction among C4 and P4 from right central and parietal regions was statistically significant. This pair of electrodes reported the strongest difference between HAHV and HALV groups. In the case of LAXV, 14 out of 496 pairs of channels were statistically significant, mainly including the interactions among right frontal region with all areas in the same hemisphere, in line with the strongest differences between LAHV and LALV depicted in Figure 5(b).

On the other hand, the maps representing XAHV and XALV approaches, Figures 5(c) HAHV-LAHV and (d) HALV-LALV, present different characteristics. If valence is fixed to a high level (Figure 5(c)), the CSE outcomes are higher (and thus the dissimilarities) for high than for low arousal in the intra- and inter-hemispheric interactions between central, temporal and parietal areas, which is represented with red colors. Differently, the relationship between left prefrontal region with all brain areas is colored with blue, which represents a more coordinated activity (lower CSE values) for high than for low arousal with a fixed high valence. In the case of a fixed low valence (Figure 5(d)), the interactions between central and temporal channels from both hemispheres, especially from the left one, with all the brain regions are colored with red, which represents a higher CSE (or higher dissimilarity) for high than for low arousal. On the contrary, the interconnections of left and right prefrontal channels and the right parietal region with all brain areas present blue colors, thus being CSE higher (lower coordination) for low than for high arousal when having a fixed low valence. This difference in the interactions between left prefrontal and all brain regions is the same as the obtained with a fixed high level of valence. In general, the differences between high and low arousal are bigger for a fixed high valence than for a fixed low valence.

In terms of the statistically significance outcomes, XAHV scheme reported 55 out of 496 statistically significant pairs of channels, with the best results in the interactions between left frontal electrodes with themselves and also with left parieto-occipital and right frontal areas. These were precisely the interactions with the strongest negative difference between HAHV and LAHV. In addition, the intra-hemispheric interactions among right fronto-central and centro-parietal channels, and the inter-hemispheric interconnections among the same areas, also presented statistically significant results, being those the regions with the highest positive differences among these two groups of emotions. With respect to XALV approach, 11 out of 496 pairs of channels were statistically significant, mainly related to the interactions among right frontal and parietal areas.

With respect to the interconnections among

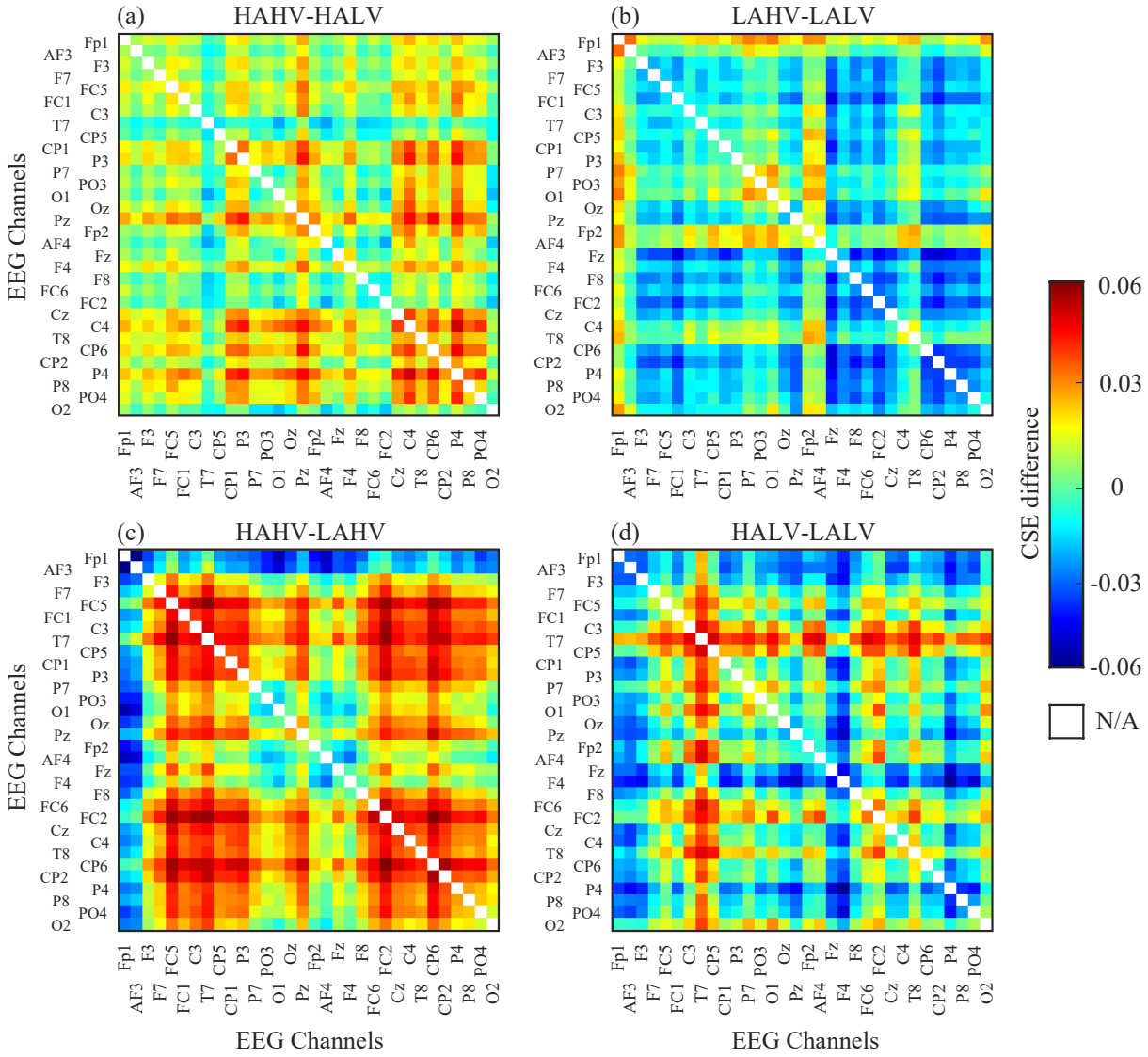

Figure 5. Difference of average levels of CSE between groups two by two in binary-class scheme. Each map represents the difference between two groups as the high level minus the low level of the variable emotional dimension (valence or arousal), having the other dimension a fixed level.

channels selected by the SFS approach for the four binary-class schemes, in the case of HAXV only the interactions among left frontal channels Fp1-AF3 and right central and parietal electrodes C4-P4 were selected by the SFS approach. The 36 pairs of electrodes selected in LAXV scheme were mainly those representing the interactions among right frontal area with central, parietal and occipital channels in the same hemisphere, in line with the statistical results reported by ANOVA. Interconnections among channels in left frontal area, on the one hand, and left parieto-occipital region, on the other hand, were also widely selected by the SFS approach. A total of 41 combinations of channels were selected in XAHV scheme, including interactions among right centro-parietal region with right fronto-central and left parietal areas, and the relations between left frontal channels with left parieto-occipital and right frontal regions. Finally, the 41 interactions selected in XALV included the connections between right frontal area with itself and with central and parietal regions from both brain hemispheres.

For each binary-class scheme, a SVM was implemented using the pairs of channels selected by the SFS approach as input features. The results of performance obtained for each binary-class approach are depicted in Table 3. As can be observed, the highest accuracy values were obtained for the schemes in which the fixed emotional dimension presented a low level, i.e., LAXV and XALV (98.20% and 97.38%, respectively). These two schemes also reported balanced results of sensitivity and specificity, thus showing similar capabilities to detect the two groups of emotions included in those binary-class schemes. The lowest classification accuracy was reported by the HAXV approach (75.54%). Precisely, this binary-class scheme presented imbalanced results of sensitivity and specificity, thus representing a good performance for the detection of only one of the two groups in this approach. Finally, XAHV scheme presented a global accuracy of 95.70%, with a difference between sensitivity and specificity of more than 80%.

Table 3. Performance of CSE in the four schemes of binary-class analysis.

Scheme	Se	Sp	Acc
HAXV	98.88%	13.86%	75.54%
LAXV	99.03%	97.18%	98.20%
XAHV	98.80%	90.32%	95.70%
XALV	95.94%	98.55%	97.38%

4. Discussion

The analysis of EEG signals with functional connectivity metrics provides interesting information about the synchronization between separate brain regions under different cognitive tasks and mental processes. In the present study, CSE has been applied for the first time to describe connectivity characteristics of the brain under emotional conditions corresponding to the four quadrants of the valence/arousal emotional space, reporting new discoveries about the coordinated activity in the emotions contained in those groups. Interestingly, CSE has already demonstrated its ability to discern between calm and distress, revealing notable insights about the synchronization of the brain under these emotional states.[17] Hence, the present manuscript reinforces the capability of CSE to identify different emotional states from EEG signals.

The computation of CSE in the present work revealed that the strongest coordinated activity appeared in the intra- and inter-hemispheric connections of parietal lobes and other posterior regions. Interestingly, the essential role of the parietal areas in emotional processes has already been highlighted. Indeed, parietal activity is related to both emotional dimensions, arousal and valence, thus providing relevant information for emotions detection.[30] Furthermore, the complementary performance of this brain region among both hemispheres has also been described under various emotional conditions.[31] On the other hand, the possible interaction among parietal and frontal areas in emotional processes has been proposed in some previous studies, suggesting the existence of both physical and functional links between those regions.[32,33] Nevertheless, the results obtained in the present study indicate that the interactions between frontal and parietal areas reported the weakest coordinated activity under the different emotional conditions studied, whereas the synchronization between other regions was higher in emotional processes.

Precisely, the interactions among parietal areas from both hemispheres with other brain regions, together with the interconnections among left and right frontal areas, reported statistically significant results when discerning between the four groups of emotions in the multiclass scheme. The CSE values of these relevant interactions were used as input features of the SVM classification model, which reported a global classification accuracy of 95.43%. This outcomes can be directly compared with other similar studies included in Table 4 in which the same database has been assessed for the detection of the four quadrants of the valence/arousal space simultaneously. As can be observed, the classification accuracy reported by the multiclass scheme in the present work is comparable with the outcomes of other studies, even overcoming these results in some cases.[34–37] Moreover, this work is focused on the assessment of a single nonlinear metric called CSE, whereas the studies with similar classification results were based on the combination of different nonlinear indices for the detection of the emotions in the four quadrants of the valence/arousal space.[38–40] In addition, it is interesting to remark that the classification process presented in

this study is based on the reduction of input features in the classifier by means of an SFS scheme. This procedure presents valuable advantages with respect to other studies given the simplification of the classification model. In addition, the preselection of the most relevant features allows to give a clinical interpretation of the classification results, since it is possible to know which are brain regions making the greatest contributions to the enhancement of the performance outcomes. Furthermore, the metric analyzed in the present study evaluates the functional connectivity and synchronization among different brain regions, thus revealing new insights about the brain behavior in emotional processes that cannot be reported by the metrics computed in the rest of works, based on the assessment of each brain area separately.

In addition, the differences between high and low levels of arousal and valence have been evaluated separately but taking into account the level of the other emotional dimension in four binary-class approaches. This scheme is different from the typical analyses for arousal and valence detection traditionally made in the scientific literature, since in most of the cases the distinction between high and low levels of one emotional dimension does not consider the state of the counterpart dimension. Nevertheless, it is known that both valence and arousal present a strong intercorrelation, hence the differentiating characteristics among high and low arousal could change depending on the level of valence, and vice versa. Therefore, the influence of one on the other makes necessary to take into account the state of both emotional dimensions even if only one of them is being evaluated.[19] Indeed, a similar scheme has already corroborated that the distinction between high and low levels of one emotional dimension is not equal when the counterpart dimension is either fixed to a high or a low level.[40]

In the case of having a fixed level of arousal, i.e., HAXV and LAXV schemes, the major differences between high and low valence were observed in the interconnections among posterior areas of the brain for both high and low fixed arousal. Nevertheless, for high arousal the synchronization in these areas was higher for low than for high valence, i.e., these regions were more coordinated for emotions in HALV (anger, fear, distress) than for HAHV (happiness, delight). This increase of synchronization could be interpreted as a mechanism of self-protection based on the enhancement of alertness for the processing of the perceived external information, preparing the body for a possible response against the negative stimuli that threaten the self-integrity of the individual.[41] However, despite visually observing differences in the maps representing the mean level of CSE for both groups of emotions, the statistical analysis and classification approach reported the lowest results, thus demonstrating more difficulties to discern between the emotional states sharing a high level of arousal, independently on their level of valence.

On the contrary, if the arousal was fixed to a low level, the interactions among these posterior areas was more coordinated for high than for low valence, hence the synchronization in these areas was higher for LAHV (relaxation, calmness) than for LALV (sadness, depression). This increase of coordination in calmness has been related to an enhancement of self-consciousness for the improvement of attention and better development of cognitive control processes.[42]

With respect to the detection of high and low arousal with a fixed valence, i.e., XAHV and XALV approaches, the synchronization in the interactions between prefrontal channels, especially in the left hemisphere, with all brain regions was greater for high than for low arousal, regardless of the fixed level of valence. In other words, these areas were more coordinated for HALV (fear, anger, distress) and HAHV (happiness, delight) than for LALV (sadness, depression) and LAHV (relaxation, calmness). Similar outcomes have been reported by previous studies also focused on the evaluation of functional connectivity in the brain under high and low levels of arousal and valence, suggesting that the brain increases the coordinated activity and coherence among prefrontal and posterior regions in high arousal situations.[43]

On the other hand, the contrary outcomes were obtained for the interactions between left temporal locations and all brain areas with fixed low valence, thus the synchronization was higher for LALV (sadness, depression) than for HALV (fear, anger, distress). The key role of the left temporal structures in depressive conditions has been already proved, highlighting an increased activation of this area and its interactions with other brain regions under negative and ruminative tendencies.[44] Another study suggested the increased inter-hemispheric coordination

Table 4. Comparison of multiclass outcomes obtained in the present work with similar previous studies for recognition of the four quadrants of valence/arousal emotional space with DEAP database.

Study	Features	Classifier	Accuracy
Zhang *et al.* (2016)[38]	EMD,[1] SE[2]	SVM	93.20%
Bagherzadeh *et al.* (2018)[39]	CD,[3] SE	PSA[4]	93.60%
Cai *et al.* (2019)[34]	ShEn,[5] SpEn[6]	LS-SVM[7]	65.13%
Gao *et al.* (2019)[35]	MSE,[8] REn,[9] FuzzEn,[10] EMD	SVM	62.01%
Soroush *et al.* (2019)[36]	Poincare planes and sections	SVM	81.67%
García-Martínez *et al.* (2021)(a)[40]	QSE,[11] AAPE,[12] PME[13]	SVM	93.75% / 96.39%
García-Martínez *et al.* (2021)(b)[37]	DispEn[14]	SVM	89.54%
Present study	**CSE**	**SVM**	**95.43%**

[1] EMD: Empirical mode decomposition
[2] SE: Sample entropy
[3] CD: Correlation dimension
[4] PSA: Parallel stacked autoencoder
[5] ShEn: Shannon entropy
[6] SpEn: Spectral entropy
[7] LS-SVM: Least square SVM
[8] MSE: Multiscale sample entropy
[9] REn: Rényi entropy
[10] FuzzEn: Fuzzy entropy
[11] QSE: Quadratic sample entropy
[12] AAPE: Amplitude-aware permutation entropy
[13] PME: Permutation min-entropy
[14] DispEn: Dispersion entropy

between temporal and frontal lobes during the processing of unpleasant stimuli.[45] Finally, the intra- and inter-hemispheric relations in frontal, central and parietal regions were more synchronized for high than for low arousal with a fixed high valence, i.e., higher for LAHV (calmness, relaxation) than for HAHV (happiness, delight). As previously mentioned, the increased coordination in a relaxed emotional state, and even during meditation processes, could be related to an improvement of the attention for the enhancement of the self-consciousness, reaching an optimum mental state for the development of cognitive tasks.[42]

However, the high level of synchronization among some areas in certain emotional states does not imply a lack of coordination between the rest of brain regions. Indeed, it is considered that there is always a minimum degree of synchronized activity among areas, although its strength and the regions involved are different depending on the requirements of the mental task that is being developed.[46] In other words, the performance of cognitive mechanisms generates a series of fluctuating patterns of synchronization among separate brain regions.[47] These coordination patterns are also present in the brain activity of an idle subject, but with a lower relevance than under the development of cognitive tasks.[48,49] Consequently, the "default system" of the brain is defined as a subset of brain areas with a stronger degree of activity under resting conditions and without paying attention to external stimuli.[50] Therefore, the brain is always synchronized, even if no relevant tasks are being executed.[51]

Notwithstanding, it is possible to find some difficulties when trying to give a physiological interpretation of the outcomes reported by metrics based on the evaluation of synchronization and coordination among brain areas. Precisely, the sensory input

of a received stimulus is firstly processed in a certain brain region, and subsequently spread to other non-connected areas for the particular treatment of the sensory information. In this sense, these regions would report a strong coordination among them. Nevertheless, it is not possible to discern whether these outcomes represent an actual synaptical association between areas or if the dynamics of both regions are similar just because of being involved in the same cognitive process originated in a common brain area. Therefore, the functional and direct connection among two areas cannot be confirmed, although it is possible to corroborate the involvement of separate brain regions in the same mental task.[48]

Finally, it is important to remark some limitations of this study. For instance, the audiovisual stimuli used in the experiment of DEAP database presented 1 minute of duration, which could be too much time for the elicitation of only one emotion, thus hindering the process of self-assessment of the individual's emotional state. On the other hand, there is no consensus about the optimal type of stimulus (e.g., images, music, videoclips...) for emotions elicitation, and the response of the brain against different options may also change. Consequently, in future works it would be interesting to analyze and compare functional connectivity of different brain regions using other types of emotional stimuli, in order to define an optimal experimental procedure for emotions elicitation. In addition, the computation in future studies of other synchronization metrics, like entropy-based symbolic indices or graph theory, could report new and complementary information to that provided by CSE. Finally, the application of advanced classification approaches based on deep learning techniques could provide valuable information about the discriminatory power of CSE and other functional connectivity metrics for the identification of different emotional states.[52,53] However, as the number of samples included in DEAP database is scarce, future experiments will also consider the necessity of including a wide number of participants and samples to allow the possibility to implement deep learning algorithms for emotions classification.

5. Conclusions

The present study has computed the CSE index for the assessment of the functional connectivity characteristics of the brain under the emotional states included in the four quadrants of the valence/arousal space. Results obtained for the four groups of emotions under study have shown a more synchronized intra- and inter-hemispheric interactions in central, parietal and occipital regions, and a lower coordination between left frontal and temporal sites with all brain structures. An ANOVA analysis for each group of emotions separately confirmed the notable difference in the level of synchronization among the aforementioned regions. Furthermore, the multiclass approach for the simultaneous assessment of the four groups of emotions under study reported a global classification accuracy of 95.43%, which overcomes the outcomes obtained in similar previous works. The differences between pairs of emotional groups were also computed in four binary-class schemes to discern between high and low levels of valence and arousal separately, but considering the state of the counterpart dimension. In this sense, outcomes have demonstrated a strong interrelation between valence and arousal, since the differences between high and low levels of one dimension changed depending on the state of the other. Concretely, the highest differences of coordination between high and low valence with fixed arousal appeared in the interactions of the right hemisphere, but with a distinct tendency depending on the fixed level of arousal. On the other hand, the prefrontal areas, especially from the left hemisphere, always presented a higher synchronization for high than for low arousal, regardless of the level of valence, although different results were obtained from the rest of brain interconnections in terms of the fixed level of valence.

Acknowledgments

This publication is part of the R&D projects PID2020-115220RB-C21, EQC2019-006063-P, funded by MCIN/AEI/10.13039/501100011033/, and 2018/11744, funded by "ERDF A way to make Europe". This work was partially supported by Biomedical Research Networking Centre in Mental Health (CIBERSAM) of the Instituto de Salud Carlos III. Beatriz García-Martínez holds FPU16/03740 scholarship from Spanish Ministerio de Educación y Formación Profesional.

Bibliography

1. J. Liu, M. Li, Y. Pan, W. Lan, R. Zheng, F.-X. Wu and J. Wang, Complex brain network analysis and its applications to brain disorders: A survey, *Complexity* **2017** (2017) p. 8362741.
2. S. Zola-Morgan, Localization of brain function: The legacy of Franz Joseph Gall (1758-1828), *Annu. Rev. Neurosci.* **18**(1) (1995) 359–383.
3. S. Anzellotti and M. N. Coutanche, Beyond functional connectivity: Investigating networks of multivariate representations, *Trends Cogn. Sci.* **22** (2018) 258–269.
4. C. O'Reilly, J. D. Lewis and M. Elsabbagh, Is functional brain connectivity atypical in autism? A systematic review of EEG and MEG studies, *PLoS ONE* **12**(5) (2017) p. e0175870.
5. V. Sakkalis, Review of advanced techniques for the estimation of brain connectivity measured with EEG/MEG, *Comput. Biol. Med.* **41**(12) (2011) 1110–1117.
6. C. Liu, B. Abu-Jamous, E. Brattico and A. K. Nandi, Towards tunable consensus clustering for studying functional brain connectivity during affective processing., *Int. J. Neural Syst.* **27** (2017) p. 1650042.
7. J. del'Etoile and H. Adeli, Graph theory and brain connectivity in Alzheimer's disease, *Neuroscientist* **23** (2017) 616–626.
8. N. Mammone, L. Bonanno, S. D. Salvo, S. Marino, P. Bramanti, A. Bramanti and F. C. Morabito, Permutation disalignment index as an indirect, EEG-based, measure of brain connectivity in MCI and AD patients, *Int. J. Neural Syst.* **27**(05) (2017) p. 1750020.
9. M. Ahmadlou, H. Adeli and A. Adeli, Spatiotemporal analysis of relative convergence of EEGs reveals differences between brain dynamics of depressive women and men., *Clin. EEG Neurosci.* **44** (2013) 175–181.
10. R. Yuvaraj, M. Murugappan, U. R. Acharya, H. Adeli, N. M. Ibrahim and E. Mesquita, Brain functional connectivity patterns for emotional state classification in Parkinson's disease patients without dementia, *Behav. Brain Res.* **298**(B) (2016) 248–260.
11. M. Ahmadlou, A. Adeli, R. Bajo and H. Adeli, Complexity of functional connectivity networks in mild cognitive impairment subjects during a working memory task, *Clin. Neurophysiol.* **125**(4) (2014) 694–702.
12. M. Ahmadlou, H. Adeli and A. Adeli, Fuzzy synchronization likelihood-wavelet methodology for diagnosis of autism spectrum disorder, *J. Neurosci. Methods* **211**(2) (2012) 203–209.
13. M. Ahmadlou and H. Adeli, Complexity of weighted graph: A new technique to investigate structural complexity of brain activities with applications to aging and autism., *Neurosci. Lett.* **650** (2017) 103–108.
14. F. Al-Shargie, U. Tariq, M. Alex, H. Mir and H. Al-Nashash, Emotion recognition based on fusion of local cortical activations and dynamic functional networks connectivity: An EEG study, *IEEE Access* **7** (2019) 143550–143562.
15. Y. Gao, X. Wang, T. Potter, J. Zhang and Y. Zhang, Single-trial EEG emotion recognition using Granger causality/transfer entropy analysis, *J. Neurosci. Methods* **346** (2020) p. 108904.
16. S. M. Pincus, Assessing serial irregularity and its implications for health, *Ann. N.Y. Acad. Sci.* **954** (2001) 245–67.
17. B. García-Martínez, A. Fernández-Caballero, R. Alcaraz and A. Martínez-Rodrigo, Cross-sample entropy for the study of coordinated brain activity in calm and distress conditions with electroencephalographic recordings, *Neural. Comput. Appl.* **33** (2021) 9343–9352.
18. J. A. Russell, A circumplex model of affect, *J. Pers. Soc. Psychol.* **39**(6) (1980) 1161–1178.
19. P. Kuppens, F. Tuerlinckx, J. A. Russell and L. F. Barrett, The relation between valence and arousal in subjective experience, *Psychol. Bull.* **139**(4) (2013) 917–940.
20. S. Koelstra, C. Muhl, M. Soleymani, J.-S. Lee, A. Yazdani, T. Ebrahimi, T. Pun, A. Nijholt and I. Patras, DEAP: A database for emotion analysis using physiological signals, *IEEE Trans. Affect. Comput.* **3**(1) (2012) 18–31.
21. G. H. Klem, H. O. Lüders, H. Jasper, C. Elger *et al.*, The ten-twenty electrode system of the International Federation, *Electroencephalogr. Clin. Neurophysiol.* **52** (1999) 3–6.
22. A. Delorme and S. Makeig, EEGLAB: An open source toolbox for analysis of single-trial EEG dynamics including independent component analysis, *J. Neurosci. Methods* **134**(1) (2004) 9–21.
23. S. Tsuchimoto, S. Shibusawa, S. Iwama, M. Hayashi, K. Okuyama, N. Mizuguchi, K. Kato and J. Ushiba, Use of common average reference and large-Laplacian spatial-filters enhances EEG signal-to-noise ratios in intrinsic sensorimotor activity, *J. Neurosci. Methods* **353** (2021) p. 109089.
24. W. W. Ismail, M. Hanif, S. Mohamed, N. Hamzah and Z. I. Rizman, Human emotion detection via brain waves study by using electroencephalogram (EEG), *Int. J. Adv. Sci. Eng. Inf. Technol.* **6**(6) (2016) 1005–1011.
25. A. Pedroni, A. Bahreini and N. Langer, Automagic: Standardized preprocessing of big EEG data, *NeuroImage* **200** (2019) 460–473.
26. J. S. Richman and J. R. Moorman, Physiological time-series analysis using approximate entropy and sample entropy, *Am. J. Physiol. - Heart Circ. Physiol.* **278**(6) (2000) H2039–H2049.
27. S. M. Pincus, Irregularity and asynchrony in biologic network signals, *Methods Enzymol.* **321** (2000) 149–82.

28. J. D. Veldhuis, S. M. Pincus, M. C. Garcia-Rudaz, M. G. Ropelato, M. E. Escobar and M. Barontini, Disruption of the joint synchrony of luteinizing hormone, testosterone, and androstenedione secretion in adolescents with polycystic ovarian syndrome, *J. Clin. Endocrinol. Metab.* **86**(1) (2001) 72–79.
29. S. J. Reeves and Z. Zhe, Sequential algorithms for observation selection, *IEEE Trans. Signal Process.* **47**(1) (1999) 123–132.
30. N. Alia-Klein, R. N. Preston-Campbell, S. J. Moeller, M. A. Parvaz, K. Bachi, G. Gan, A. Zilverstand, A. B. Konova and R. Z. Goldstein, Trait anger modulates neural activity in the frontoparietal attention network, *PLoS ONE* **13**(4) (2018) p. e0194444.
31. H. Saarimäki, A. Gotsopoulos, I. P. Jääskeläinen, J. Lampinen, P. Vuilleumier, R. Hari, M. Sams and L. Nummenmaa, Discrete neural signatures of basic emotions, *Cereb. Cortex* **26**(6) (2016) 2563–2573.
32. R. J. Davidson, Affect, cognition, and hemispheric specialization, *Emotion, Cognition, and Behavior*, (Cambridge University Press, New York, 1988), pp. 320–365.
33. A. Martínez-Rodrigo, B. García-Martínez, R. Alcaraz, P. González and A. Fernández-Caballero, Multiscale entropy analysis for recognition of visually elicited negative stress from EEG recordings, *Int. J. Neural Syst.* **29**(02) (2019) p. 1850038.
34. J. Cai, W. Chen and Z. Yin, Multiple transferable recursive feature elimination technique for emotion recognition based on EEG signals, *Symmetry* **11**(5) (2019) p. 683.
35. Gao, Cui, Wan and Gu, Recognition of emotional states using multiscale information analysis of high frequency eeg oscillations, *Entropy* **21** (2019) p. 609.
36. M. Z. Soroush, K. Maghooli, S. K. Setarehdan and A. M. Nasrabadi, Emotion recognition through EEG phase space dynamics and Dempster-Shafer theory, *Med. Hypotheses* **127** (2019) 34–45.
37. B. García-Martínez, A. Fernández-Caballero, R. Alcaraz and A. Martínez-Rodrigo, Application of dispersion entropy for the detection of emotions with electroencephalographic signals, *IEEE Trans. Cogn. Develop. Syst.* (2021).
38. Y. Zhang, X. Ji and S. Zhang, An approach to eeg-based emotion recognition using combined feature extraction method, *Neurosci. Lett.* **633** (2016) 152–157.
39. S. Bagherzadeh, K. Maghooli, J. Farhadi and M. Z. Soroush, Emotion recognition from physiological signals using parallel stacked autoencoders, *Neurophysiology* **50**(6) (2018) 428–435.
40. B. García-Martínez, A. Fernández-Caballero, L. Zunino and A. Martínez-Rodrigo, Recognition of emotional states from EEG signals with nonlinear regularity-and predictability-based entropy metrics, *Cognit. Comput.* **13**(2) (2021) 403–417.
41. G. G. Knyazev, Cross-frequency coupling of brain oscillations: An impact of state anxiety, *Int. J. Psychophysiol.* **80**(3) (2011) 236–245.
42. A. Barrós-Loscertales, S. E. Hernández, Y. Xiao, J. L. González-Mora and K. Rubia, Resting state functional connectivity associated with Sahaja Yoga Meditation, *Front. Hum. Neurosci.* **15** (2021) p. 65.
43. R. Cao, Y. Hao, X. Wang, Y. Gao, H. Shi, S. Huo, B. Wang, H. Guo and J. Xiang, EEG functional connectivity underlying emotional valance and arousal using minimum spanning trees, *Front. Neurosci.* **14** (2020) p. 355.
44. M. A. Ferdek, C. M. van Rijn and M. Wyczesany, Depressive rumination and the emotional control circuit: An EEG localization and effective connectivity study, *Cogn. Affect. Behav. Neurosci.* **16**(6) (2016) 1099–1113.
45. N. Martini, D. Menicucci, L. Sebastiani, R. Bedini, A. Pingitore, N. Vanello, M. Milanesi, L. Landini and A. Gemignani, The dynamics of EEG gamma responses to unpleasant visual stimuli: From local activity to functional connectivity, *NeuroImage* **60**(2) (2012) 922–932.
46. H.-J. Park and K. Friston, Structural and functional brain networks: From connections to cognition, *Science* **342**(6158) (2013) p. 1238411.
47. C. Schmidt, D. Piper, B. Pester, A. Mierau and H. Witte, Tracking the reorganization of module structure in time-varying weighted brain functional connectivity networks., *Int. J. Neural Syst.* **28** (2018) p. 1750051.
48. J. L. P. Velazquez, R. G. Erra, R. Wennberg and L. G. Dominguez, *Coordinated activity in the brain* (Springer, New York, USA, 2009), ch. Correlations of Cellular Activities in the Nervous System: Physiological and Methodological Considerations, pp. 1–24.
49. L. Cheng, Y. Zhu, J. Sun, L. Deng, N. He, Y. Yang, H. Ling, H. Ayaz, Y. Fu and S. Tong, Principal states of dynamic functional connectivity reveal the link between resting-state and task-state brain: An fMRI study., *Int. J. Neural Syst.* **28** (2018) p. 1850002.
50. R. L. Buckner, J. R. Andrews-Hanna and D. L. Schacter, The brain's default network: Anatomy, function, and relevance to disease., *Ann. N.Y. Acad. Sci.* (2008).
51. M. D. Fox, A. Z. Snyder, J. L. Vincent, M. Corbetta, D. C. Van Essen and M. E. Raichle, The human brain is intrinsically organized into dynamic, anticorrelated functional networks, *Proc. Natl. Acad. Sci.* **102**(27) (2005) 9673–9678.
52. U. R. Acharya, S. L. Oh, Y. Hagiwara, J. H. Tan, H. Adeli and D. P. Subha, Automated EEG-based screening of depression using deep convolutional neural network, *Comput. Methods Programs Biomed.* **161** (2018) 103–113.
53. U. Raghavendra, U. R. Acharya and H. Adeli, Artificial intelligence techniques for automated diagnosis of neurological disorders, *Eur. Neurol.* **82** (2019) 41–64.